

REPORT DOCUMENTATION PAGE			Form Approved OMB No. 0704-0188	
<small>Public reporting burden for this collection of information is estimated to average 1 hour per response, including the time for reviewing instructions, searching existing data sources, gathering and maintaining the data needed, and completing and reviewing the collection of information. Send comments regarding this burden estimate or any other aspect of this collection of information, including suggestions for reducing this burden, to Washington Headquarters Services, Directorate for Information Operations and Reports, 1215 Jefferson Davis Highway, Suite 1204, Arlington, VA 22202-4302, and to the Office of Management and Budget, Paperwork Reduction Project (0704-0188), Washington, DC 20503.</small>				
1. AGENCY USE ONLY (Leave blank)		2. REPORT DATE 24 Feb 98	3. REPORT TYPE AND DATES COVERED FINAL: 16 SEP 96 - 15 SEP 97	
4. TITLE AND SUBTITLE "SYNTHESIS AND CHARACTERIZATION OF CONDUCTING ELASTOMERS BASED ON INTERPENETRATED C 60-DERIVED POLYMER NETWORKS"			5. FUNDING NUMBERS G - F49620-96-1-0473	
6. AUTHOR(S) PROFESSOR LONG Y. CHIANG PROFESSOR LEE Y. WANG				
7. PERFORMING ORGANIZATION NAME(S) AND ADDRESS(ES) THE FOUNDATION OF CONDENSED MATTER SCIENCES NATIONAL TAIWAN UNIVERSITY 1 ROOSEVELT ROAD TAIPEI, TAIWAN			8. PERFORMING ORGANIZATION REPORT NUMBER N/A	
9. SPONSORING/MONITORING AGENCY NAME(S) AND ADDRESS(ES) ASIAN OFFICE OF AEROSPACE RESEARCH AND DEVELOPMENT (AOARD) UNIT 45002 APO AP 96337-5002			10. SPONSORING/MONITORING AGENCY REPORT NUMBER AOARD 96-06	
11. SUPPLEMENTARY NOTES				
12a. DISTRIBUTION AVAILABILITY STATEMENT APPROVED FOR PUBLIC RELEASE; DISTRIBUTION IS UNLIMITED.			12b. DISTRIBUTION CODE	
13. ABSTRACT (Maximum 200 words) <p>Highly stretchable elastomers embedded with a thin conducting polyaniline layer. A processing technique was demonstrated for the fabrication of interpenetrating conductive polyaniline networks at the near-surface region of fullereneol hypercrosslinked poly (urethane ether) elastomer films. The resulting conductive elastomer film is highly stretchable and exhibits appreciable conductivity in the incorporated, doped polyaniline layer without deteriorating the elasticity and tensile strength of the bulk supporting polymer. Conductive polymers designed by this synthetic method exhibit increased conductivity even upon elastomer elongation by 500% of original length. Hysteresis was observed; however, a high reversibility of the strain-dependent resistivity was evident, thus indicating no further deterioration in the strain-dependent resistance. Also, full compressibility of the conductive C60-PU-PANI elastomer with a nearly constant pressure-dependent resistance was observed from 10 psi to 90 psi.</p> <p>Synthesis of octadecahydroxylated C70. Novel hydrophilic {70} polymers were synthesized in a reaction involving oxidative sulfation of the C70 molecules induced by H2SO4-SO3. Addition of P205 or SeO2 achieved modulation of the sulfation rate with high yield (72%). MALDI-TOF mass spectrum of the {70} fullerenols indicate octadecahydroxyfullerenes containing 18 hydroxy addends per C70 cage, which correlates the structure of its sulfated precursor as noncyclosulfated {70} fullerene, C70(SO4)9.</p>				
14. SUBJECT TERMS Conducting polymers, synthesis of conducting polymers, conductive polymer and elastomeric polymer composites, polymer/elastomer chemistry.			15. NUMBER OF PAGES 30	
			16. PRICE CODE	
17. SECURITY CLASSIFICATION OF REPORT UNCLASSIFIED	18. SECURITY CLASSIFICATION OF THIS PAGE UNCLASSIFIED	19. SECURITY CLASSIFICATION OF ABSTRACT UNCLASSIFIED	20. LIMITATION OF ABSTRACT UL	

19980618 020

**SYNTHESIS AND CHARACTERIZATION OF CONDUCTING
ELASTOMERS BASED ON INTERPENETRATED
C₆₀-DERIVED POLYMER NETWORKS**

Long Y. Chiang

*Center for Condensed Matter Sciences, National Taiwan University
Taipei, Taiwan*

**A Report Submitted to AOARD/AFOSR for the Research Contract under
the Grant No. FQ8671-9601280**

PART I

Highly Stretchable Elastomers Embedded with a Thin Conducting Polyaniline Layer

Lee Y. Wang and Long Y. Chiang*

Center for Condensed Matter Sciences, National Taiwan University, Taipei, Taiwan

Abstract: A synthetic procedure was developed for the preparation of interpenetrating conductive polyanilines at the near-surface region of the fullerenol (dodecahydroxylated C_{60}) hypercrosslinked poly(urethane-ether) elastomers. The resulting conductive elastomers exhibit a room-temperature conductivity of 2.6 Scm^{-1} in the interpenetrated, doped polyaniline layer without deteriorating elasticity and tensile strength of the bulk supporting C_{60} -derived elastomer. The strain-dependent conductivity profile of this conductive elastomer was found to decrease slightly within 50% elongation, followed by a steady increase to a maximum value of 5.4 Scm^{-1} at 430% elongation of the film prior to break. During the same experiment, the surface resistance of elastomer expanded from $2.4 \text{ k}\Omega$ to $33 \text{ k}\Omega$ at 430% elongation of the film. This synthetic method illustrated a feasible approach in the design of conducting elastomers, showing an increase of conductivity even after the elastomer being elongated to a length as much as 500% of its original size. By using a pulling rate of 1.0 mm/min on a conductive elastomer film of 6 mm in length with application of a reversible strain force equivalent to a maximum elongation length of 10–50% of its original size, a hysteresis in the first strain cycle was observed. After the second strain cycle, a high reversibility of the strain-dependent resistivity was evident, showing all strain-dependent resistance data fitted in a confined loop without further deterioration. Furthermore, a full compressibility of the conductive C_{60} -PU-PANI elastomer with a nearly constant pressure-dependent resistance was observed from 10 psi up to 90 psi .

Introduction

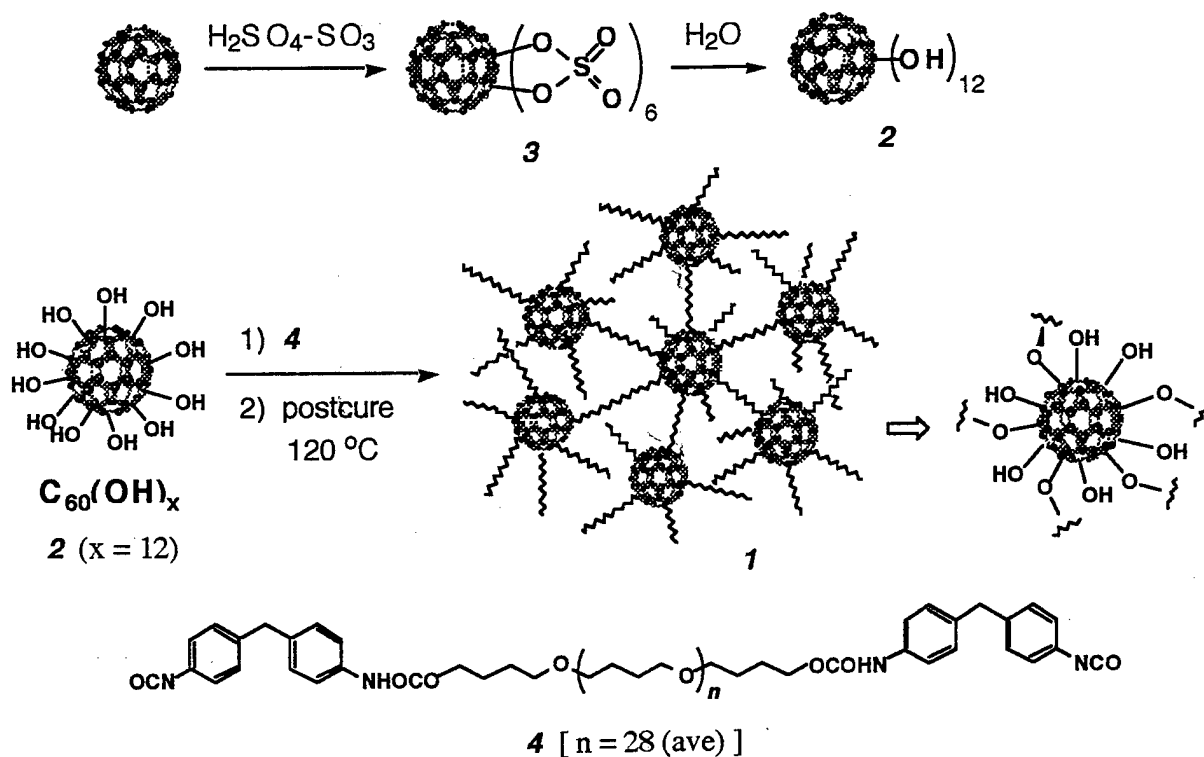
Electrochemical deposition of conducting polymers onto the surface of an electrode, coated with a thin film of the insulating hosting polymer, in the presence of electrolytes was demonstrated as an early method¹ for the synthesis of conductive polymer blends with a moderate conductivity

of $10\text{--}100\text{ Scm}^{-1}$. The most widely used approach to combine electronic conductivities with the desirable mechanical strength of polymers in a large-scale preparation of conductive blends is to make a direct blending of conductive polymers with soluble polymers or thermoplastics.²⁻¹⁴ However, incompatibility of conducting polymers with the hosting polymer matrix, causing irreversible phase-separation or aggregation of microparticles, and the significantly reduced conductivity of final products continue to be major problems for this blending method. Meanwhile, the tendency of conductive particles to migrate has also created inconsistency in electronic performance of these blends.

Interfacial polymerization,¹⁵ emulsion polymerization,^{14,16} and *in situ* polymerization of conductive monomer precursors thus become potentially important methods in producing technologically valuable blends. Incorporation of the rigid rod-like conducting polymer guest inside an elastic polymer matrix often alters significantly the intrinsic physical and mechanical properties of the parent host polymer. A sharp increase of modulus and toughness was observed in an elastomer blended with conductive polymers in a concentration as low as 10%.¹⁷ Therefore, in favor of retaining elasticity of the hosting polymer, it is necessary to limit the quantity of conducting polymer used in the blend to well below 10%. In this case, a low content of conducting polymers in the bulk phase of blend below the critical concentration for a continuous conducting path within the matrix may result in a low conductivity of the blend upon application of a strain force. One way to holding a high conductivity while maintaining a low level of conductive components in the blend is to localize all conductive molecules within a thin layer across the supporting matrix. A high composition ratio of conductive polymers in this thin layer should lead to an appreciable conductivity along the layer. Using this approach, coexistence of conductivity and elasticity may be conceivable in one elastomeric material.

To achieve a continuous well-defined conductive layer within a host matrix material, we have recently demonstrated a synthetic method for embedding a thin polyaniline layer along the near-surface region inside an elastomer film.¹⁸ The resulting film product was found to be highly stretchable with a conductivity comparable to that of the doped bulk polyanilines. The method involved an *in situ* polymerization of aniline inside an elastomer network forming the interpenetrated polyaniline rods across flexible soft segments of the elastomer. With a fine control of oxidant diffusion, polymerization of aniline can be restricted exclusively at the near-surface region within a hosting polymer, leaving the rest of bulk matrix relatively free of polyaniline particles. Specifically, the chemistry resulted in the formation of elastic conductive composites which consisted of a dodecahydroxylated C_{60} hypercrosslinked poly(urethane-ether) network (1, C_{60} -PU) and a thin layer of interpenetrated network (IPN) of polyaniline (PANI). During the extensive materials characterizations, for the first time, we investigated the reversibility of the

strain-dependent and pressure-dependent conductivity properties of these newly synthesized C_{60} -derived conductive elastomers containing polyanilines.



Scheme 1: Synthesis of polyhydroxylated C_{60} hypercrosslinked poly(urethane-ether) network (1, C_{60} -PU) as the parent elastomeric matrix.

Experimental Section

General. Infrared spectra were recorded as KBr pellets on a Nicolet 750 series FT-IR spectrometer or a JASCO FT-IR-300E spectrometer. ^1H NMR spectra were recorded on a Varian Gemini-300 or a Bruker AM-300WB spectrometer. Dynamic mechanical analyses (DMA) were performed on a DuPont 983 dynamic mechanical analyzer at a frequency of 1 Hz and a heating rate of $5\text{ }^{\circ}\text{C}$ per min with specimen 3 cm long and 1 cm wide. DSC, TGA, and TMA data were collected on TA instruments equipped with a DSC 2910 differential scanning calorimeter, a TGA 2950 thermogravimetric analyzer, and a TMA 2940 thermal mechanical analyzer, respectively. TGA-FTIR data were collected on a TGA 2950 thermogravimetric analyzer which was interfaced with a Nicolet 750 series FT-IR spectrometer at a heating rate of $6\text{ }^{\circ}\text{C}$ per min. All other mechanical properties of polymers were performed on a Tensilon RIM-IT universal testing instrument using the ASTM D412/75 standard with a 33 mm x 6 mm x 2 mm specimen and a rate

of material extension fixed at 20 cm per min. Poly(tetramethylene oxide) glycol (PTMO) was purchased from DuPont de Nemours Co. and used as received. 4,4'-Diphenylmethane diisocyanate (MDI) and 2,2-dichloroethanol were purchased from Tokyo Kasei Chemicals. Benzene and toluene were dried and distilled over Na. Purification and dehydration of dimethylformamide was carried out by filtration through a column packed with BaO, followed by distillation under vacuum and drying over molecular sieves (4Å). Elemental analyses of fullerenols and polymers were carried out at National Cheng Kung University, Taiwan. A Sintech 2G Universal Mechanical Testing System (MTS) equipped with both an ammeter and a voltmeter for the online conductivity measurements was used for the study of reversibility of the strain-dependent and pressure-dependent conductivity of the dodecahydroxylated C₆₀-derived conducting elastomers containing polyanilines.

Synthesis of dodecahydroxylated fullerenes 2 (fullerenols). A modified reaction procedure for the synthesis of hexacyclosulfated fullerene derivatives from the reported literature was used.¹⁹ A reaction flask (50 ml) charged with a fullerene mixture of C₆₀ (84%) and C₇₀ (16%) (1.0 g) (or pure C₆₀) and fuming sulfuric acid (15 ml) was stirred at 55-60 °C under N₂ for 3 days to give a dark brown solution with orange suspensions. The resulting mixture was added dropwise into anhydrous diethyl ether (200 ml, distilled over CaH₂) with vigorous stirring in an ice bath to cause the precipitation of products. Precipitates were separated from solution by the centrifuge technique. They were then washed and centrifuged three times with anhydrous diethyl ether and twice with 2:1 anhydrous diethyl ether-CH₃CN, and dried in vacuum at 40 °C to afford brown-orange solids of hexacyclosulfated fullerenes 3 (1.3 g). The physical data of the hexacyclosulfated fullerenes are as follows: IR ν_{max} (KBr) 2920 (br), 2400 (br), 1706 (w), 1654 (w), 1598 (w), 1426 (s), 1233 (s), 1168, 1046, 1002 (s), 981, 953 (s), 855, 826 (s), 783, 641, 530, 485 (w), and 411 (w); ¹³C NMR (DMF-*d*₇, peak center) δ 148.0, 77.0, 71.0; ¹H NMR (DMF-*d*₇, peak center) δ 14.6 (w, OSO₂-OH). Elemental analyses: C, 59.13; H, 0.93; O, 25.46; S, 12.02; XPS (atomic %): C, 67.7; O, 26.6; S, 4.8.

A reaction flask (50 ml) equipped with a condenser and an inert gas bubbler was charged with hexacyclosulfated fullerenes (500 mg) and distilled water (10 ml). The mixture was stirred at 85 °C under N₂ for 10 h to give a dark brown suspension. The suspended solids were separated from aqueous solution by the centrifuge technique. The solids were repeatedly washed with water and centrifuged, then dried in vacuum at 40 °C to afford brown solids of dodecahydroxylated fullerenes 2 (fullerenols, 405 mg, 80% overall yield from C₆₀). The physical data of compound 2

are as follows: IR ν_{max} (KBr) 3317 (br, s, OH), 1623, 1381, 1049 (s), and 607; ^1H NMR (DMF- d_7 , peak center) δ 4.85 (OH); ^{13}C NMR (DMF- d_7 , peak center) δ 148.0, 81.0, 76.0. Elemental analyses: C, 69.07; H, 2.51; O, 23.82; XPS (atomic %): C, 79.9; O, 20.0; S, 0.09.

Synthesis of dodecahydroxylated fullerenes (fullerenols) derived poly(urethane-ether) network 1. Prior to the reaction, 4,4'-diphenylmethane diisocyanate (MDI) was treated at 70 °C for 2 h and poly(tetramethylene oxide) glycol (PTMO) was partially dehydrated under vacuum for at least 8 h. A three-necked reaction flask was charged with poly(tetramethylene oxide) glycol (M_n 2000, 50 g) and 4,4'-diphenylmethane diisocyanate (13.1 g, 2:1 equiv.). The mixture was stirred at 65 °C under N_2 to effect the condensation reaction of isocyanate functions with PTMO glycols. Progress of the condensation reaction was monitored by detection of the decrease in intensity of both infrared bands centered at 3320 and 2272 cm^{-1} corresponding to the absorption of hydroxy and isocyanate functions, respectively. The resulting diisocyanated poly(urethane-ether) prepolymer **4** was used directly without further separation and purification. Fullerenols **2** (936 mg) were dissolved in DMF (15 mL) and dried in the presence of molecular sieves (4Å). The DMF solution was then transferred via syringe into a reaction flask containing diisocyanated poly(urethane-ether) prepolymer **4** (15 g, 1.0 equiv. of NCO group per OH in fullereneol) in DMF (60 ml, dried over molecular sieves) to give a solution containing 16% by weight of fullereneol. The mixture was stirred at ambient temperatures for 1.5 h. The reaction was continued in a glove-box at ambient temperatures for a period of 16 h under N_2 . Termination of the reaction was carried out by quenching the product intermediates with methanol. The residual solvent was removed at 70 °C under vacuum for 24 h. The resulting elastomeric films were separated from the surface of the reaction container by slow diffusion of distilled H_2O at the interface between the film and glass surfaces. After the evaporation of H_2O , dodecahydroxylated fullerene-derived poly(urethane-ether) networks **1a** were obtained as dark red films. Infrared spectra of **1a** were ν_{max} (ATR) 3500 (br, OH), 3302 (br, s, NH), 2939 (s), 2854 (s), 2796, 1731, 1710, 1649, 1598, 1536, 1513, 1483, 1447, 1413, 1367, 1310, 1221, 1103 (s), 1018, 984, 962, 817, 769, and 668.

In a separated polymerization reaction, the quantity of diisocyanated poly(urethane-ether) prepolymer **4** applied was half (7.5 g, 0.5 equiv of NCO group per OH in fullereneol) of that used in the preparation of **1a**, giving a closely related dodecahydroxylated fullerene-derived poly(urethane-ether) networks **1b** as a dark red film. Infrared spectra of **1b** were ν_{max} (ATR) 3500 (br, OH), 3302 (br, s, NH), 2940 (s), 2854 (s), 2797, 2742, 1731, 1712, 1650, 1599, 1536, 1513, 1484, 1447, 1413, 1367, 1310, 1221, 1104 (s), 1018, 985, 817, 769, and 669.

Synthesis of polyaniline interpenetrated conducting elastomers. In a typical reaction, the elastomer **1a** or **1b** was immersed in a THF solution containing aniline (50% by volume) overnight to afford an aniline-swollen elastomer film. It was then dried in vacuum at ambient temperature for 30 min to remove THF. Polymerization of aniline was initiated by allowing the elastomer film into contact with an aqueous oxidant solution, containing LiCl (2.3 M), $(\text{NH}_4)_2\text{S}_2\text{O}_8$ (0.055M), and HCl (0.5M). After a reaction period of 14 h at -15°C , the resultant film was washed repeatedly with water and THF in a sequence and then treated with a solution of ammonium hydroxide (1 M) in THF for 2 h to neutralize protonated polyanilines to their emeraldine base form. The film was rinsed repeatedly with *N*-methyl-pyrrolidone (NMP) for removal of physically adsorbed or deposited polyanilines from the surface. Conductive form of the elastomer can be made by redoping the film with HCl (2 N) in THF and dried in vacuum for 24 h at ambient temperature to afford the conducting polyaniline interpenetrated fullereneol-polyurethane elastomer **5** (C_{60} -PU-PANI). IR (ATR) ν_{max} (KBr) 3434 (br, s, OH), 1631, 1387, 1065, and 472; ^{13}C NMR (THF- d_8 , the highest peak of band) δ 147.4, 146.0, 143.2, 72.0–84.0 (very weak).

Results and Discussion

Several moldable or extractable conducting blends have been made by mixing or permeating conductive polypyrrole or polyaniline²⁰ with either thermoplastics of PVC, PETG, and nylon 12 or elastomeric terpolymers of ethane, propene and 5-vinylnorborn-2-ene (as EPDM).²¹ In the latter case, incorporation of the rigid rod-like conducting polymers inside the elastomeric polymer matrix often decreases significantly the elasticity of parent supporting elastomers.

In our approach to synthesize conductive polymer composites, exhibiting crucial mechanical properties, an *in situ* polymerization of conducting polymer precursors within the supporting polymer matrix was applied. This can be accomplished by first incorporating polymerizable monomers inside the supporting matrix followed by a controlled diffusion of oxidative catalysts into the matrix to effect the polymerization, or vice versa. The supporting matrix used in this study was an elastomer of fullereneol crosslinked poly(urethane-ether) network (**1**, C_{60} -PU), where dodecahydroxylated C_{60} (fullereneol, **2**)¹⁹ was utilized as a hypercross-linking agent,^{22,23} which exhibit high elasticity, high tensile strength, and low T_g . The approach resembles the use of fullereneol as a molecular core in the building of star-shaped polymers.²⁴

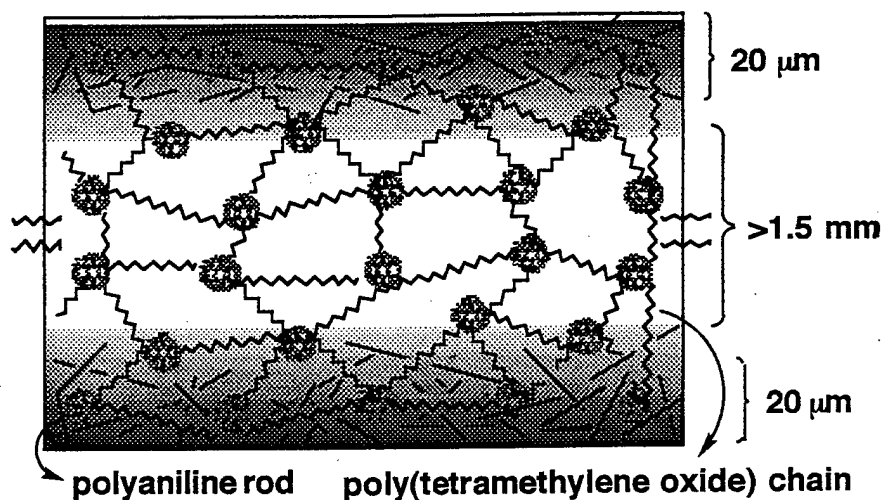


Figure 1: Schematic presentation of the polyaniline-interpenetrated poly(urethane-ether) network (1, C_{60} -PU) which was crosslinked by dodecahydroxylated C_{60} .

One synthesis of fullerenols **2** was carried out by hydrolysis of hexacyclosulfated fullerenes, which were products resulted from the reaction of C_{60} with oleum [$H_2SO_4-SO_3$ (28–30%)] at 60 °C for a period of 12 h to 3 d depending on the C_{60} vs oleum ratio by weight used.¹⁹ A slow dissolution of C_{60} into the acid medium in an over-saturated mixture can deter the efficient oxidation of C_{60} and prolong the reaction period. We found that cyclosulfation of the fullerene molecules, using oleum as an oxidative sulfation reagent, in a fully dissolved state can be greatly accelerated to complete within a reaction period of 80 min at 60 °C upon the addition of P_2O_5 (8.5 equiv.), as a secondary oxidation promoter. This reaction is both dose and temperature dependent. Thus, the period required for a complete reaction was shortened to 40 or 20 min when 17 or 34 equiv. of P_2O_5 , respectively, was applied under similar reaction conditions. As the reaction temperature being increased to 80 °C with an application of P_2O_5 (17 equiv.), a complete sulfation reaction was achieved within as short as 5–10 min.

Reaction of the fullerene molecules with oleum involved a SO_3 -induced stoichiometric electron oxidation of C_{60} and its analogous, forming the cationic radical intermediates of fullerenes which were stabilized under strong acidic conditions. Proceeding of this radical formation can be followed readily by a visual change of the reaction mixture to a dark brownish green solution, containing suspended unreacted fullerene particles if any. Existence of the fullerenic radicals in solution was substantiated by detection of an absorption peak in its *e.s.r.* spectrum.^{25,26} The attack of the resulting cationic intermediates by nucleophilic anionic sulfate species, such as HSO_4^- and $HS_2O_7^-$ (as a product of HSO_4^- and SO_3), afforded the corresponding cyclosulfated

fullerenes **3** which precipitated out from the acid solution as orange-red solids, as shown in Scheme 1. Removal of sulfuric acid was made by transferring the resulting acid suspension dropwise into a mixture of anhydrous diethylether and acetonitrile/1:2 to further effect precipitation of dissolved **3**. Hydrolysis of **3** in water at 85 °C gave fullerenols **2** in an overall yield of roughly 80–87% from C₆₀.

Characteristics of fullerenic cyclosulfate moieties in **3** were noticed in its infrared spectrum displaying two sharp, strong absorptions centered at 1426 and 1229 cm⁻¹, corresponding to the asymmetric RO–SO₂–OR stretch and symmetric RO–SO₂–OR stretch bands, respectively. Both the absorption intensity and the peak position of these two bands were found to agree well with those of –SO₂– absorptions reported for hexacyclosulfated C₆₀ synthesized by the reaction of C₆₀ with H₂SO₄–SO₃ in the absence of P₂O₅.¹⁹ Hexacyclosulfated C₆₀ **3** was readily hydrolyzable in H₂O at 85 °C to afford dodecahydroxylated fullerene **2**. Contrarily, the hydrolysis rate of **3** at 0 °C was found to be very limited. Therefore, it becomes possible to apply chilly ice-water for brief washings and removal of sulfuric acid from the reaction medium during the purification of **3**. The infrared spectrum of **2** exhibited five characteristic broad absorption bands centered at 3366, 1624, 1384, 1045, and 558 cm⁻¹ in close resemblance to those reported for fullerenols.¹⁹

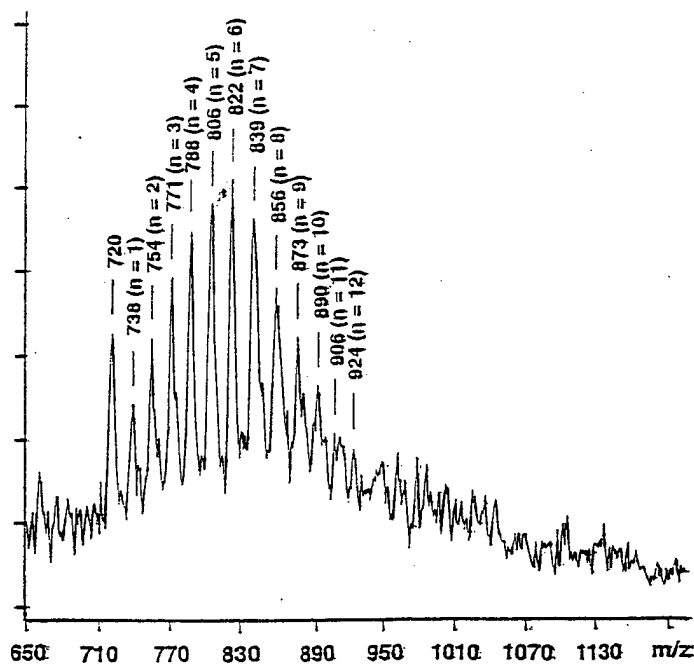


Figure 2: Positive ion MALDI-MS spectrum of **2**, derived from **3** which was synthesized under a sulfation temperature of 70 °C for 12 h in the presence of oleum–P₂O₅, displaying a fragmentation pattern consistent with a mass of dodecahydroxylated fullerene.

The mass spectroscopic studies were carried out using the matrix-assisted laser desorption ionization (MALDI) technique with either sinapinic acid or 2,5-dihydroxybenzoic acid as a matrix material. As a result, the MALDI-MS spectrum of **2** (Fig. 2), derived from **3** prepared under a sulfation temperature of 70 °C for 12 h in the presence of oleum-P₂O₅, displayed a series of mass groups with a well-defined pattern of a nearly constant weight increase in 17 mass units at m/z (the mass of an ion fragmentation with a maximum peak intensity in each group) 738 ($n = 1$), 754 ($n = 2$), 771 ($n = 3$), 788 ($n = 4$), 806 ($n = 5$), 822 ($n = 6$), 839 ($n = 7$), 856 ($n = 8$), 873 ($n = 9$), and 890 ($n = 10$), except m/z 906 ($n = 11$) and 924 ($n = 12$) with a less intensity. These ion fragmentations showing the gain of a hydroxy (OH) functional group to the preceding ion fragment agrees well with the mass of a formula of C₆₀(OH)_{*n*}, as polyhydroxylated C₆₀ derivatives. That clearly indicated a composition of the fulleranol molecule **2**, containing up to 12 hydroxy addends per C₆₀ cage (dodecahydroxyfullerene).

A modified synthetic procedure was utilized for the preparation of fulleranol-derived elastic networks used in this study. The chemical reactivity of tertiary fullerenic hydroxy group in **2** toward isocyanate functions was found to surpass that of **2** with several reactive condensative reagents studied, including organic acid chloride. Consequently, compound **2** was utilized as an active component in its reaction with diisocyanated derivatives yielding the corresponding urethanic polymers. Quantitative reaction of **2** with diisocyanated oligomers allows the treatment of its function as a hypercrosslinking agent for the preparation of various networks. Whereas fulleranol has a much higher number of reactive functions per unit volume of crosslinking center than that of conventional crosslinkers. Experimentally, the synthesis of diisocyanated oligo(urethane-ether) **4** was carried out by the reaction of poly(tetramethylene oxide) glycol (PTMO) with 4,4'-methane diphenyl diisocyanate (MDI, 2.1 equiv.) in CDCl₃ at 60 °C under N₂. The average molecular weight of poly(tetramethylene oxide) glycol used was determined to be M_n 2,000 and M_w 4,500 with a polydispersity of 2.25. When diisocyanated oligo(urethane-ether) **4** was treated with more than two equivalents of methanol, the resultant oligo(urethane-ether) bisurethanes had a chemical composition with a carbon to nitrogen ratio of 29.8. That revealed a chemical structure of poly(tetramethylene oxide) glycol containing roughly 29 repeating units of tetramethylene oxide consistent with the molecular weight of PTMO as 2150 Dalton. Similar results were obtained by calculating the integration ratio between peaks, in the ¹H NMR spectrum of methanol-terminated **4**, corresponding to aromatic protons in urethanic moieties at δ 7.1 and 7.3 and aliphatic protons in PTMO moieties at δ 1.6 and 3.4.

The high compatibility of fulleranol with water limits the total removal of water from its reaction medium. Prior to the reaction, fullereneols were dried in vacuum at 60 °C overnight,

followed by molecular sieves (4 Å) in anhydrous DMF. Under these dehydration conditions, the content of water in the fullerenol solution was estimated to be less than 0.5% by wt. The condensation reaction between diisocyanated oligo(urethane-ether) **4** and partially hydrated fullerenols was performed in anhydrous DMF at ambient temperatures under N₂ for 16 h. Gradual gel formation was observed during the first few hours of reaction. Progression of the condensation reaction was monitored by the progressive decrease in intensity of the isocyanatic absorption bands centered at 2270 cm⁻¹, the decrease in intensity of the hydroxy absorption bands centered at 3480 cm⁻¹, and the increase in intensity of the urethanic absorption bands at 3300 and 1733 cm⁻¹ in the infrared spectrum of the reaction intermediates. At the end of the reaction period, unconverted isocyanates were allowed to react terminately under the ultrasonic treatment with an excess of methanol or 2,2'-dichloroethanol, which was applied as a chlorinated end-group for assisting the elemental analysis and the quantification of free dangling polymer arms in the network. After the removal of volatile or soluble components from the reaction products, the resultant fullerenol hypercrosslinked polyurethane networks **1a** (6.0 equiv. of **4** per fullerenol molecule used) and **1b** (3.0 equiv. of **4** per fullerenol molecule used) were isolated as the solid elastomeric films.

In this condensation reaction, a limited quantity of water solvated around the fullerenol molecules has a salient effect on physical properties of the resulting polymer products. Evidently, water molecules exhibit competitive reactivity in contact with isocyanate functions at temperatures above 40 °C, as compared with that of fullerenolic alcohol. Therefore, deviation of the structure of the polymer products and their physical properties from those of the fullerenol-isocyanate condensed products prepared under anhydrous conditions becomes significant at temperatures above 60 °C. Above that temperature, reproducibility of the fullerenol-derived elastomers depends greatly on the quantity of water molecules present in the reaction medium. Presumably, the reaction of water molecules with one equivalent of isocyanate group produces the corresponding *para*-substituted aniline function. Further reaction of the *para*-substituted aniline function with another equivalent of isocyanate group affords an urea moiety, which enhances possible cross-linking at appreciably high temperatures. That serves as the mechanistic origin of the structural variation of the networks **1** prepared at temperatures above 60 °C. In the case of condensation reactions performed at ambient temperatures, the reproducible, controllable fullerenol-derived elastomeric products were achieved in excellent yields, based on the quantity of fullerenol used.

The infrared spectrum of **1** showed the disappearance of a band around 2272 cm⁻¹, corresponding to the absorption of isocyanate NCO groups. It also showed a significant decrease in the intensity of hydroxy absorption bands, as compared with that of fullerenols, centered at

3550 cm^{-1} . The conversion of isocyanate functions into the corresponding urethanes was evident by observation of the infrared bands centered at 3300 and 1733 (strong) cm^{-1} , corresponding to the urethanic NH and carbonyl absorptions, respectively. Elucidation of the chemical structure of fulleranol-derived polyurethane network was performed by means of various spectroscopic measurements and elemental analyses. The solid state ^{13}C NMR spectra of **1a** and **1b** showed two strong peaks at δ 27 and 71, corresponding to alkane (C-C) and oxygenated (C-O) carbons, respectively. In addition to peaks of the aromatic carbons of benzene rings in the urethanic moieties at δ 110–160, networks **1a** and **1b** also displayed peaks of the fullerenic carbons centered at δ 135 as a broad band. To facilitate the determination of the number of oligo(urethane-ether) chains covalently attached on each fulleranol cage, the residual, unconverted isocyanate groups present in the structure of condensation intermediates were quenched with 2,2'-dichloroethanol at the end of reaction. Thus, the resultant network containing terminally chlorinated carbons can be analyzed and quantified for its chlorine contents, which correlates in principle to the number of dangling oligo(urethane-ether) chains inside the product network. As a result, elemental analyses of both networks **1a** and **1b** showed a chlorine to nitrogen ratio of 0.14, on average, indicating a structure of **1** consisting of one 2,2'-dichloroethanol-terminated, dangling oligo(urethane-ether) arm per 2.5 covalently bonded, nondangling oligo(urethane-ether) chains. That corresponds well to 70% of flexible poly(urethane-ether) chains being crosslinked with fullereneols at both chain-ends and a 30% of them being attached to fullereneol cages at one chain-end only. In a separate experiment, the network **1a** was allowed to react thermally in the thermogravimetric analyzer which was equipped with a FT-IR spectrometer. The onset temperature for cleavage of the urethanic C-O bonds in **1a** was observed to be 300 $^{\circ}\text{C}$. At this temperature, the sole detection of CO_2 evolution as shown by the infrared absorption bands centered at 2440 cm^{-1} in the spectrum was indicative of this bond cleavage. The loss of weight was then increased with the increase of temperature to 370 $^{\circ}\text{C}$. In this temperature region, the weight loss corresponds, presumably, to the elimination of urethanic moieties. At temperatures above 400 $^{\circ}\text{C}$, a sharp raise of weight loss was detected. The infrared absorption bands of volatiles vaporized within this narrow temperature range corresponds to the combined absorptions of urethane, CO_2 , and PTMO moieties. The elimination of PTMO chains from **1a** was nearly complete as the temperature reached 520 $^{\circ}\text{C}$, showing mainly a spectrum of CO_2 . The continuing evolution of CO_2 at higher temperatures may be attributed to the bond cleavage of the oxygenated fullerene cores. The remaining residues were found to consist of 10% by weight of materials at 600 $^{\circ}\text{C}$. Considering all possible fragmentations of fullereneol cages in **1a**, the final weight of carbon residues may be utilized in the calculation of the number of PTMO chains per fullereneol

molecule in the network matrix. This number was estimated to be 8–10 which is slightly higher than the number of polymer arms (6) chemically attached on the fullerene cage of its star-burst polymer analogues synthesized previously.²⁴ Apparently, the network **1** contains tangled, unremovable linear poly(urethane-ether) chains even after repeated cleaning of **1** with THF.

Structurally, the flexible poly(tetramethylene oxide) segments serve as major chemical components in the solid matrix of **1**. Therefore, their dominative contribution to the thermal properties of **1** can be expected. We found that the lineshape of differential scanning calorimetric (DSC) profiles of **1** adheres largely to the process of thermal annealing prior to the measurement. The initial heating cycle of **1a** displayed a clear glass transition at $-70\text{ }^{\circ}\text{C}$ which was followed by an exothermic recrystallization of soft-chain segments at $-34\text{ }^{\circ}\text{C}$ (9.9 J/g) and a major endothermic chain-softening transition at $6\text{ }^{\circ}\text{C}$ (20.3 J/g). Subsequent to a slow recrystallization transition of urethanic PTMO segments at $23\text{ }^{\circ}\text{C}$ (30.2 J/g) in the first cooling cycle, the exothermic heat of the recrystallization transition in the second and the third heating cycles was fully minimized. Both the glass transition at $-69\text{ }^{\circ}\text{C}$ and the PTMO chain-softening transition at $14\text{ }^{\circ}\text{C}$ (22.5 J/g) were found to stabilize following the annealing treatment during the first cooling cycle from $200\text{ }^{\circ}\text{C}$. For the purpose of comparison, a linear polymer analogue to **1** as a model compound of poly(urethane-ether) was synthesized by the reaction of 1,4-butanediol (1.0 equiv) with diisocyanated PTMO oligomers **4** at $60\text{ }^{\circ}\text{C}$ under an atmospheric pressure of N_2 . Interestingly, we found that incorporation of fullerene molecules for hypercrosslinkings of the urethanic poly(tetramethylene oxide) chains within the materials matrix did not lead to significant alteration of the glass transition of each individual poly(tetramethylene oxide) urethane chain. As indicated in its temperature-dependent DSC profiles, the glass transition temperature of **1a** was found in the similar temperature range as that of **1b** ($-71\text{ }^{\circ}\text{C}$). A thermal transition at $8\text{ }^{\circ}\text{C}$ (14.0 J/g), corresponding to the chain-softening temperature of urethanic poly(tetramethylene oxide) segments of polymers **1b**, were detected to be slightly higher than that of **1a**. These data implied that the segmental motion of each PTMO chain covalently interconnected among C_{60} molecules in networks tends to dominate the thermal characteristics of the material that exhibits rather limited influence by the density of crosslinking at low temperatures. When the temperature was increased gradually above its glass transition, the effect of crosslinking is still barely detectable. However, the temperature-dependent loss modulus (E'') of these polymer films in the dynamic mechanical analyses (DMA) indicated a larger shift of the glass transition temperature going from linear polyurethane at $-78\text{ }^{\circ}\text{C}$ to the fullerene crosslinked network **1b** at $-64\text{ }^{\circ}\text{C}$, and then to the network **1a** at $-56\text{ }^{\circ}\text{C}$. The clear shift of T_g from a lower temperature for a linear polymer to a higher one for **1a** agrees well with the

increase of the number of crosslinking sites at each crosslinking center. A higher degree of crosslinking reduces the tight packing among urethanic poly(tetramethylene oxide) chains making them meltable (softening) at a slightly lower temperature. In addition, the temperature dependency of storage modulus (E') of both **1a** and **1b** showed a continuous raise of modulus below T_g with a modulus of 213 and 194 Mpa, respectively, at T_g . At temperatures above $-30\text{ }^{\circ}\text{C}$, the storage modulus remained constant as the temperature increased to the limit of DMA measurements. Apparently, the fulleranol hypercrosslinked systems provided the extended stability in a temperature region well beyond their T_g .

Thermal mechanical properties of **1a** were studied using a flat-point probe under a constant force of 0.05N. An increase of dimensions of the elastomer film slightly more than its linear temperature-dependent thermal expansion was observed at an onset temperature of approximately $-70\text{ }^{\circ}\text{C}$, consistent with its glass transition temperature. The rate of increase in the dimensions of the polymer was then largely suppressed when the temperature reached the recrystallization transition at $-34\text{ }^{\circ}\text{C}$. The chain-softening transition of PTMO at $6\text{ }^{\circ}\text{C}$ induced a sharp increase in the dimensions of the polymer. It was followed by a linear thermal expansion at higher temperatures. In some cases, an additional sharp increase of elastomer dimensions much more than its linear thermal expansion was observed at an onset temperature of $110\text{ }^{\circ}\text{C}$ prior to the thermal penetration of the polymer film by a pressurized probe at $195\text{ }^{\circ}\text{C}$ for **1a** or at $190\text{ }^{\circ}\text{C}$ for **1b**. Following those temperatures, a rapid decline in dimensions of the polymer film indicated the spontaneous mechanical failure of material at this thermal transition, which was undetectable in DSC measurements.

The tensile strength of polymers at break was found to be 13.8 and 11.2 MPa for **1a** and **1b**, respectively. The tensile strength of a polymer network can be modulated by variation of the crosslinking density within the matrix. In principle, an elastomeric material containing a higher density of crosslinking may enhance its tensile strength accordingly. The observed higher tensile strength of **1a** over that of pentaerythritol-crosslinked polyurethane, as a model elastomer, is therefore consistent with the estimated number of crosslinked PTMO arms per fulleranol cage in **1a** being higher than 4.0, which is the number of crosslinking sites per pentaerythritol molecule in the model elastomer. The elongation at break of **1a** and **1b** were measured to be 540% and 460%, respectively, in a similar range to that of the model elastomer (600%).

In a separate system, water molecules were fully removed from the reaction medium prior to the condensation reaction between fulleranol and the diisocyanated PTMO oligomers **4** by a tedious dehydration procedure, including the repeated drying of all reaction media and reagents with molecular sieves. The analogues fulleranol-hypercrosslinked polyurethane elastomers **1**

prepared under such anhydrous conditions exhibited mechanical tensile strength at break, elongation at break, and modulus of elasticity of 7.2 MPa, 580%, and 4.8 Mpa, respectively. The glass transition temperature of the network was found to be $-71\text{ }^{\circ}\text{C}$ as estimated from its DSC profile, and $-66\text{ }^{\circ}\text{C}$ as determined from the temperature-dependent loss modulus profile of dynamic mechanical analyses. Relating these thermal and mechanical data to those of **1a** and **1b**, an increase in tensile strength, modulus, and T_g by 92%, 83%, and $10\text{ }^{\circ}\text{C}$ (based on the DMA data), respectively, favorable for the elastomer **1a** can be realized. These increases in materials properties correlated well with a higher crosslinking density in the matrix of **1a**. Apparently, a trace quantity of water molecules present in the synthesis of **1a** contributed effectively to the increase of the density of crosslinking.

During the study of *in situ* polymerization of aniline, an additional postcuring process at $120\text{ }^{\circ}\text{C}$ was used. The resultant elastomeric networks **1** was then immersed in an aniline-containing THF solution to afford an aniline-swollen polymer matrix. After removal of THF, the film was allowed into contact with an aqueous oxidant solution, containing LiCl (2.3 M), $(\text{NH}_4)_2\text{S}_2\text{O}_8$ (0.055 M), and HCl (0.5 M), at -10 to $-20\text{ }^{\circ}\text{C}$ for 14 h. Polymerization of aniline, initiated by the surface-diffused persulfate salt, can be followed as the color of film changed from dark red to dark blue and then green. An excess of aniline and persulfate salt were removed by successive washings with water, followed by THF. Residual polyanilines, at their emeraldine base form, physically attached on the surface of the product **5** were cleaned by repeatedly rinsing with *N*-methyl-2-pyrrolidinone (NMP) and THF.

Surface characterization is crucial to allow differentiation between the physical coating and the interpenetrated networking of PANI at the surface of **5**. The former gives predominately spectroscopic characteristics of PANI and the latter should provide a combined absorption spectrum of PANI and poly(urethane-ether) (PUE). Thus, the infrared attenuated total reflection (ATR) spectroscopic studied were applied for the determination of relative, proportional functional compositions at the surface of an elastomer film **5**. With a proper calibration of the infrared peak intensity and the peak area ratio between peaks using blends of PANI, in its emeraldine base form, and linear poly(urethane-ether) in a known ratio, the detected ATR intensity can be correlated to a relative chemical composition. This intensity correlation was examined and the results were depicted in Fig. 3. Two absorption bands centered at 1300 and 1237 cm^{-1} were used for the investigation. A monotonic increase of the peak area ratio of a band at 1300 cm^{-1} to a band at 1237 cm^{-1} was observed as the polyaniline composition in the blend increases. It reaches a maximum value of 3.92 for pure polyaniline [Fig. 3(f)] and a minimum value of 0.31 for pure poly(urethane-ether) [Fig. 3(a)]. The correlation curve was made by plotting the weight fraction of polyaniline

versus the peak area ratio, followed by fitting these data points with a quadratic polynomial equation. By inserting the observed peak area ratio (1.6) of the IPN elastomer **5** into the correlation curve, a PANI composition of 40%, which corresponds to a weight ratio (wt. of PANI/wt. of PUE) of 0.67, was obtained. Since the ATR spectrum measures the optical absorption of functions at the surface of a film, results indicated a relative surface composition of **5** as (PUE)_{1.0}(PANI)_{0.67} by weight in addition to the dispersed fullerene cages (5.0% by weight).

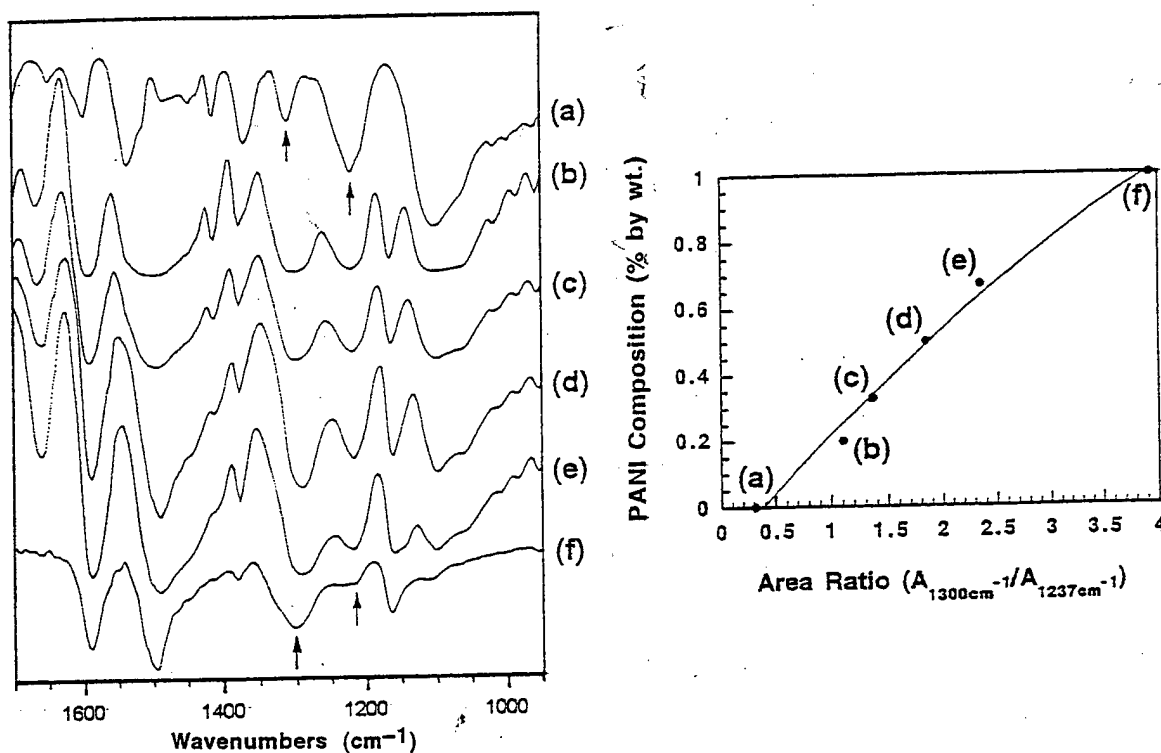


Figure 3: Correlation study of the peak intensity to functional compositions at the surface by means of Infrared ATR absorptions of poly(urethane-ether) (PUE) and undoped polyaniline (PANI) blends in a weight ratio (PUE to PANI) of (a) 100:0, (b) 80:20, (c) 66:33, (d) 50:50, (e) 33:66, and (f) 0:100.

Microscopic studies of the thinly sliced cross-section of an elastomer film **5** showed clearly a dark green-blue layer of PANI dispersed within the film matrix. The layer was measured to be roughly 20 μm in thickness and extended from the surface boundary of elastomer, as shown in Fig. 4. Remarkably, the bulk interior region of the elastomer film was found to be nearly free of PANI. By applying the thickness of this conductive PANI layer in the calculation of resistivity using a four-point probe technique, the room-temperature conductivity of **5** was found to be 2.6 Scm^{-1} . The elongation at break of **1** and **5** was measured to be $550 \pm 20\%$ and $430 \pm 20\%$, respectively. Apparently, there is only a limited change of maximum elongation at break upon

incorporation of a thin PANI layer into **1**. Since interpenetration of the conducting PANI is restricted exclusively to a region of 20 μm in the surface of a film about 0.5 mm or more in thickness, retention of the most of bulk physical properties in the resulting products is anticipated.

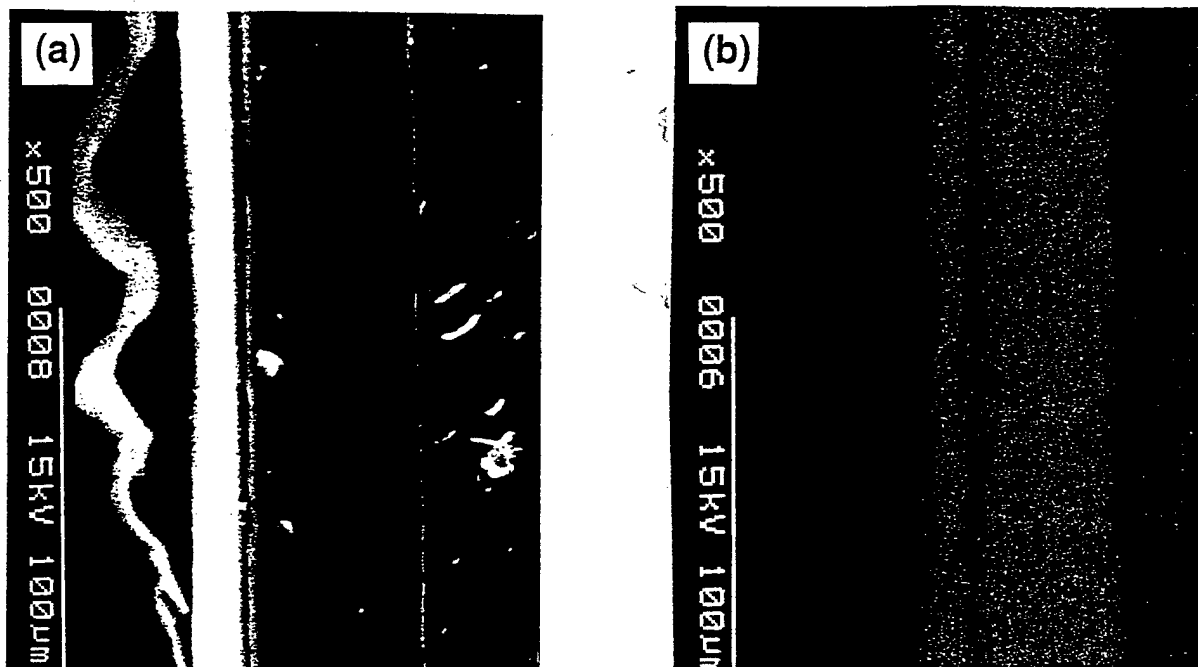


Figure 4: Electron probe X-ray micrograph (EPMA) of conducting polyaniline incorporated fullerenol-linked poly(urethane-ether) elastomer **5** (a) showing a polyaniline-PU layer in a thickness of roughly 20 microns at the near-surface region of **5** and (b) the chlorine mapping of the cross-section of the matrix indicating a similar thickness of the layer.

One of the most important physical properties of conducting elastomers is the strain-dependent conductivity. It was measured under a constant strain rate of 1 mm per min and plotted versus the elongation (%) of film, as shown in Fig. 5. This conductivity profile of **5** was found to decrease slightly within 50% elongation $[(L - L_0) / L_0]$ of the elastomer, followed by steadily increase to a maximum of 5.4 Scm^{-1} at 430% of film elongation prior to break. During the same experiment, the surface resistance (R) of **5** expanded from 2.4 $\text{k}\Omega$ to 33 $\text{k}\Omega$ at 430% elongation of the film. As the elastomer film is stretched under force, the cross-section area (A) of the conducting layer changes inversely proportional to the change of length (L) between conducting probes. Therefore, the conductivity (σ) can be obtained by the following equation, $\sigma = L^2 / (R \times L_0 \times A_0)$, where L_0 and A_0 are the initial length between conducting probes and the initial cross-

section area of the conducting layer, respectively, before stretching. The fact of the conductivity increase of **5** to approximately double of its initial value, when the film was extended to 5.3 times of its original length, strongly indicated the rigid rod-like polyaniline chains being microscopically dispersed and interpenetrated inside the elastomer matrix instead of being aggregated as the individual PANI particles. This is consistent with the polymer morphology shown in the scanning electron micrograph of the sliced cross-section of film **5** shown in Fig. 4. In cases of the conductive blends containing aggregated PANI particles, the percolation threshold plays a major role in limiting the long-range electron transporting path that normally results in a sharp decline of conductivity upon stretching of the specimen. The initial conductivity decrease of the IPN network **5** at low elongation is presumably due to the physical reorganization and sliding of the PANI polymer chains in the host matrix in response to the external strain force. It is feasible to interpret that the observed moderate conductivity increase at high elongation may arise from the increase in electron tunneling efficiency among PANI chains when these PANI chains in an IPN system are pressed into contact with each other as a result of the strain-induced reduction of the film dimension perpendicular to the stretching direction.

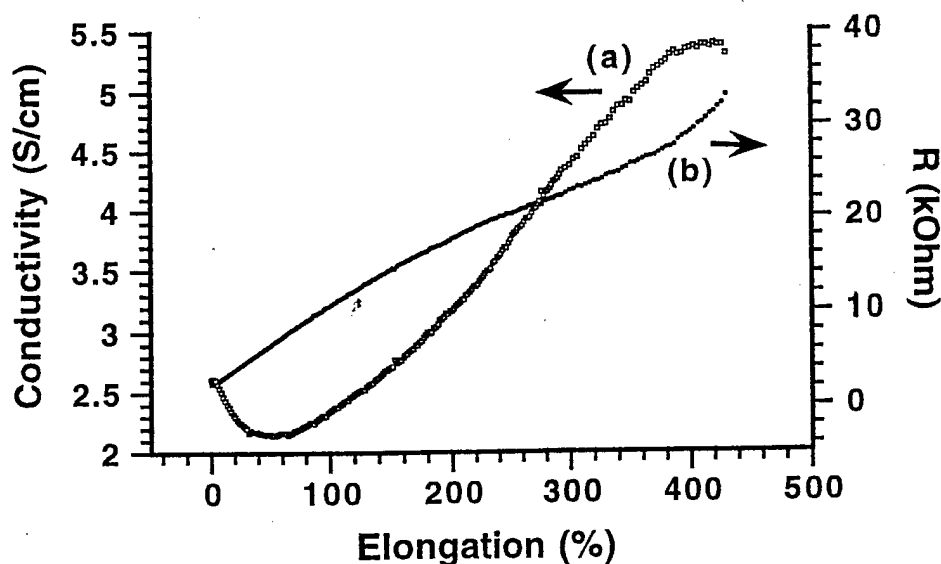


Figure 5: Strain-dependent conductivity (a) and resistance (b) profiles of a fullereneol-derived conducting elastomer interpenetrated with polyaniline chains at the near-surface region as a layer of 20 μm in thickness.

Reversibility of the strain-dependent conductivity of dodecahydroxylated C_{60} -derived conducting elastomers **5** was investigated. A Sintech 2G Universal Mechanical Testing System (MTS) equipped with both an ammeter and a voltmeter for the online conductivity measurements was used for the study. As a result, when a low strain force equivalent to a maximum elongation

length of 10% of its original size was applied reversibly, a slow increase of resistance from 4.5 k Ω to 5.6 k Ω was observed initially prior to the release of strain force. Owing to the fact that the actual relaxation rate of the matrix elastomer is much lower than the change of the strain force releasing rate (1.0 mm/min) during the conductivity measurements, the C₆₀-PU-PANI film **5** may not be fully relaxed back to its original position in-time for the next cycle measurement. Therefore, a progressive small increase of resistance was detected as compared with that of the preceding cycle, as shown in Fig. 6. As the strain force was increased to a value equivalent to a maximum elongation length of 50% of its original size reversibly, as shown in Fig. 7, a larger dimension change of the matrix film led to a corresponding larger increase of resistance as compared with that observed in Fig. 6. By using the same pulling rate of 1.0 mm/min, a similar hysteresis in the first strain cycle was observed. That shifted the resistance value upward from 60 k Ω to 160 k Ω at a 0.5 mm extension length on a sample film of 6 mm in length in the second strain cycle. After the second strain cycle, a high reversibility of the strain-dependent resistivity was evident, showing all strain-dependent resistance data fitted in a confined loop without further deterioration.

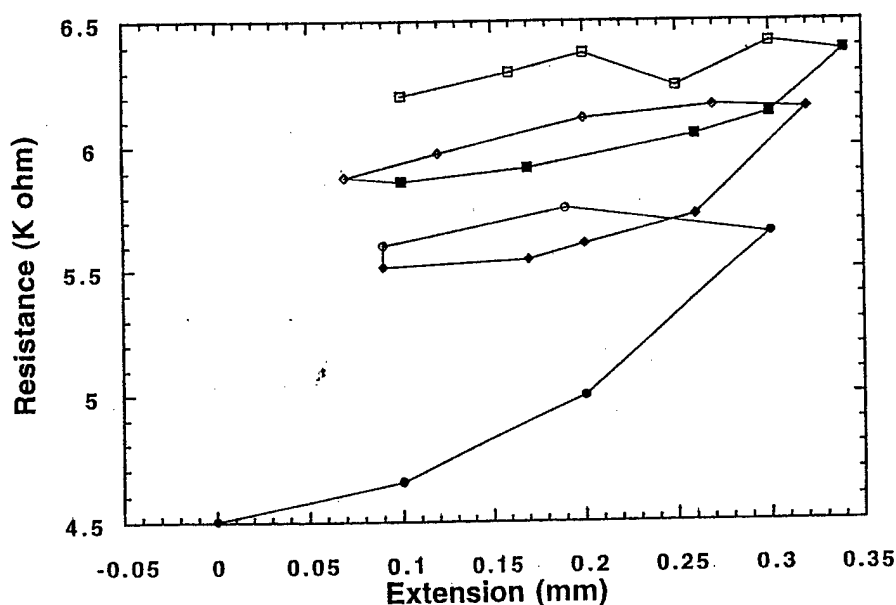


Figure 6: Strain-dependent resistance profiles of a fullereneol-derived conducting elastomer interpenetrated with polyaniline chains **5**, showing a good reversibility of resistance upon application of a low strain force with a maximum of 10% elongation.

A similar technique was utilized for the study of compressibility of the pressure-dependent resistance on the conductive fullereneol-derived polyurethane-polyaniline elastomer **5**. As depicted in Fig. 8, the variation of resistance of a sample film in all measurements was found to be rather small, between 0.67 and 0.71 k Ω , upon the application of pressure from 10 psi up to 90 psi. Considering the fluctuation level and the difficulty of these conductivity measurements, the

observed small variation of the pressure-dependent resistance may be regarded as a neglectible value. That can be interpreted into a full compressibility of the conductive C_{60} -PU-PANI elastomer **5** with a nearly constant pressure-dependent resistance up to 90 psi.

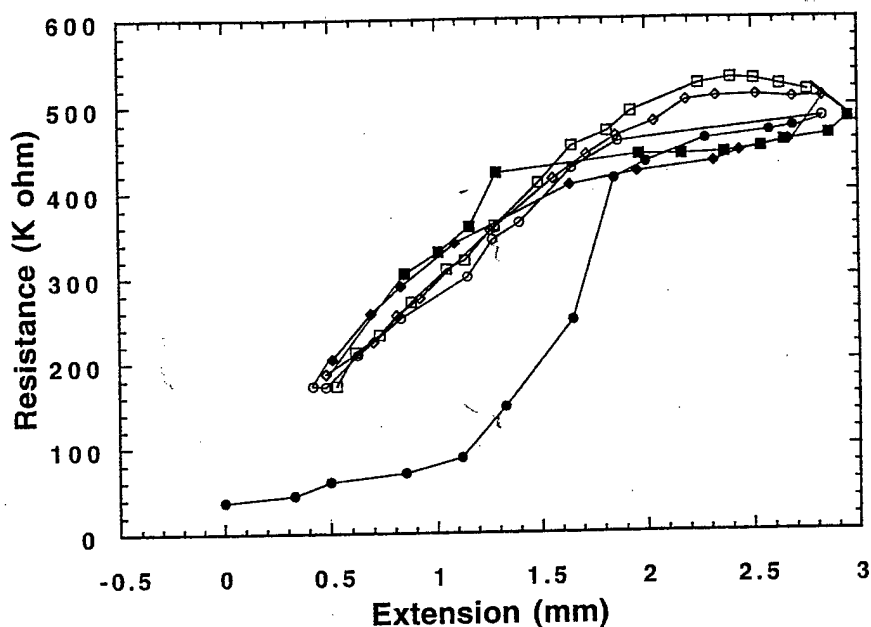


Figure 7: Strain-dependent resistance profiles of a fullerene-derived conducting elastomer interpenetrated with polyaniline chains **5**, showing a good reversibility of resistance upon application of a medium strain force with a maximum of 50% elongation.

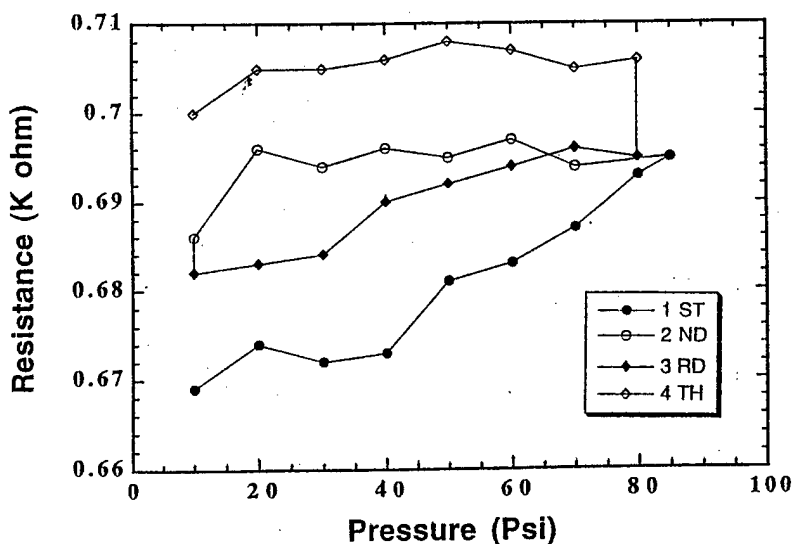


Figure 8: Pressure-dependent resistance profiles of a fullerene-derived conducting elastomer interpenetrated with polyaniline chains **5**, showing a good reversibility of resistance upon application of pressure with a maximum compression pressure of 90 psi.

Conclusion

We demonstrated a processing technique for the fabrication of interpenetrating conductive polyaniline networks at the near-surface region of the fullereneol hypercrosslinked poly(urethane-ether) elastomers. The resulting conductive elastomers exhibit an appreciable conductivity in the incorporated, doped polyaniline layer without deteriorating the elasticity and tensile strength of the bulk supporting polymer. This synthetic method illustrated a feasible approach in the design of conducting elastomers, showing an increase of conductivity even after the elastomer being elongated to a length as much as 500% of its original size. By using the same pulling rate of 1.0 mm/min on a conductive elastomer film of 6 mm in length with application of a strain force equivalent to a maximum elongation length of 10–50% of its original size reversibly, a hysteresis in the first strain cycle was observed. After the second strain cycle, a high reversibility of the strain-dependent resistivity was evident, showing all strain-dependent resistance data fitted in a confined loop without further deterioration. Furthermore, a full compressibility of the conductive C₆₀-PU-PANI elastomer with a nearly constant pressure-dependent resistance was observed from 10 psi up to 90 psi.

Acknowledgment. This work was supported partially by AOARD/AFOSR under the grant no. FQ8671-9601280.

References

- (1) De Paoli, M. A.; Waltman, R.; Diaz, A.; Bargon, J. *J. Polym. Sci., Polym. Chem. Ed.* **1985**, *23*, 1687.
- (2) Galvin, M. E.; Wnek, G. E. *Polymer* **1982**, *23*, 795.
- (3) Tripathy, S. K.; Rubner, M. F. *Polymers in Electronics*; T. Davidson, Ed.; Am. Chem. Soc., Washington, DC, 1984; p 48.
- (4) Andreatta, A.; Heeger, A. J.; Smith, P. *Polym. Commun.* **1990**, *31*, 275.
- (5) Wessling, B. *Adv. Mater.* **1991**, *3*, 507.
- (6) Beadle, P.; Armes, S. P. *Macromolecules* **1992**, *25*, 2526.
- (7) Zinger, B.; Behar, D.; Kijel, D. *Chem. Mater.* **1993**, *5*, 778.
- (8) Ikkala, O. T.; Laakso, J.; Vakiparta, K.; Virtanen, E.; Ruohonen, H.; Jarvinen, H.; Taka, T.; Passiniemi, P.; Osterholm, J. E.; Cao, Y.; Andreatta, A.; Smith, P.; Heeger, A. J. *Synth. Met.* **1995**, *69*, 97.
- (9) Im, S. S.; Byun, S. W. *J. Appl. Polym. Sci.* **1994**, *51*, 1221.

- (10) Shacklette, L. W.; Han, C. C.; Luly, M. H. *Synth. Met.* **1993**, 55-57, 3532.
- (11) Liu, C. F.; Maruyama, T.; Yamamoto, T. *Polym. J.* **1993**, 25, 363.
- (12) Kathirgamanathan, P. *Polymer* **1993**, 34, 2907.
- (13) Chen, S. A.; Lee, H. T. *Macromolecules* **1995**, 28, 2858.
- (14) Yang, S.; Ruckenstein, E. *Synth. Met.* **1993**, 59, 1.
- (15) Nakata, M.; Kise, H. *Polym. J.* **1993**, 25, 91.
- (16) Osterholm, J. E.; Cao, Y.; Klavetter, F.; Smith, P. *Synth. Met.* **1993**, 55-57, 1034.
- (17) De Paoli, M. A.; Maia, D. J. *J. Mater. Chem.* **1994**, 4, 1799.
- (18) Chiang, L. Y.; Wang, L. Y.; Kuo, C. S.; Lin, J. G.; Huang, C. Y. *Synth. Met.* **1997**, 84, 721.
- (19) Chiang, L. Y.; Wang, L. Y.; Swirczewski, J. W.; Soled, S.; Cameron, S. *J. Org. Chem.* **1994**, 59, 3960.
- (20) Kulkarni, V. G.; Mathew, W. R.; Wessling, B.; Merkle, H.; Blaettner, S. *Synth. Met.* **1991**, 41-43, 1009.
- (21) Zoppi, R. A.; Felisberti, M. I.; De Paoli, M. A. *J. Polym., Sci., Part A, Polym. Chem.* **1994**, 32, 1001.
- (22) Chiang, L. Y.; Wang, L. Y.; Kuo, C. S. *Macromolecules* **1995**, 28, 7574.
- (23) Wang, L. Y.; Wu, J. S.; Kuo, C. S.; Tseng, S. M.; Hsieh, K. H.; Chiang, L. Y. *J. Polym. Res.* **1996**, 3, 1.
- (24) Chiang, L. Y.; Wang, L. Y.; Tseng, S. M.; Wu, J. S.; Hsieh, K. H. *J. Chem. Soc., Chem. Commun.* **1994**, 2675.
- (25) S. G. Kukolich and D. R. Huffman, *Chem. Phys. Lett.*, 1991, **182**, 263.
- (26) (a) H. Thomann, M. Bernardo and G. P. Miller, *J. Am. Chem. Soc.*, 1992, **114**, 6593; (b) G. P. Miller, C. S. Hsu, H. Thomann, L. Y. Chiang and M. Bernardo, *Mater. Res. Soc. Symp. Proc.*, 1992, **247**, 293.

PART II

SYNTHESIS OF OCTADECALHYDROXYLATED C_{70}

Boy-Horn Chen^a, Jen-Pang Huang^b, Lee Y. Wang^c, Jentaie Shiea^b,
Tun-Li Chen^a and Long Y. Chiang^{c,*}

^aDepartment of Chemistry, Tamkang University, Taipei, Taiwan.

^bDepartment of Chemistry, Sun Yat-sen University, Kaohsiung, Taiwan.

^cCenter for Condensed Matter Sciences, Taiwan University, Taipei, Taiwan.

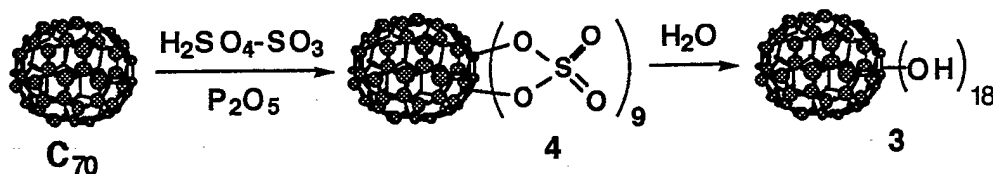
Abstract: Synthesis of novel hydrophilic [70]fullerenols was described. The reaction involved an oxidative sulfation of the C_{70} molecules induced by $H_2SO_4-SO_3$. The rate of sulfation was accelerated either moderately or greatly by the addition of P_2O_5 or SeO_2 , respectively, with a product yield of 86%. Hydrolysis of the resulting cyclosulfated C_{70} in H_2O at 80 °C afforded [70]fullerenols in a yield of more than 72%. The MALDI-TOF mass spectrum of [70]fullerenols clearly indicated their composition as octadecahydroxyfullerenes, containing 18 hydroxy addends per C_{70} cage. That correlates the structure of its sulfated precursor as nonacyclosulfated [70]fullerene, $C_{70}(SO_4)_9$.

Introduction

Addition of multiple hydroxy functions onto a fullerene cage enhances its water-compatibility. A C_{60} molecule containing more than 18 hydroxy groups was found to be water-soluble¹⁻⁴. Dodecahydroxylated C_{60} is the sole [60]fullerenol analogous molecule soluble in either DMF and a mixture of DMF-THF⁵. The organic solubility makes its uses possible in the synthesis of star-burst polymers⁶ and in the preparation of highly elastic polymer materials, as a hypercrosslinking agent for enhancement of the tensile strength and other mechanical properties^{7,8}. In addition, polyhydroxylated fullerenes were reported to be useful as an antioxidant in removing biologically active oxygen species⁹ against the oxidative stress mediated cell damages¹⁰ and diseases¹¹. It is, therefore, of our interest to investigate the hydroxylation chemistry of the C_{70} molecules.

Results and Discussion

Dodecahydroxylated C_{60} **1**, $C_{60}(OH)_{12}$, was first synthesized via hydrolysis of hexacyclosulfated C_{60} **2**, which was the main reaction product of C_{60} with fuming sulfuric acid⁵. Progress of the latter reaction can be accelerated to completion within few hours of reaction at 60 °C in the presence of P_2O_5 . The mass of the molecular ion of dodecahydroxylated C_{60} and the related ion fragmentations were detected in its MALDI-TOF (matrix assisted laser desorption ionization) mass spectrum profile¹². Sulfation of C_{60} with fuming sulfuric acid was proposed to involve a sequential stoichiometric electron oxidation of C_{60} , induced by SO_3 as an initiation step of the reaction, followed by trapping of the resulting cationic C_{60} intermediates with anionic sulfate species^{5,13}.



Scheme 1: Synthesis of octadeca-hydroxylated C_{70} ([70]fullerenols)

A similar sulfation mechanism is expected for the synthesis of polycyclosulfated C_{70} molecules. However, a much slower reaction rate of derivatization of the C_{70} molecules by the oxidative sulfation was observed as compared with that of C_{60} . It required normally a reaction period of more than 3 d for a complete sulfation of C_{70} in neat oleum at 60 °C.

We found that this sulfation rate can be improved, to a lesser extend than that for the C_{60} molecules, upon the application of P_2O_5 as an oxidation enhancer. As an example, it may take a slightly less than 40 h to complete sulfation of C_{70} at ambient temperatures in the presence of P_2O_5 (130 equiv.) with a reaction yield of 70%. As the reaction temperature increases, the sulfation rate was detected to increase in a temperature-dependent fashion, as shown in Fig. 1. The period of reaction time necessary for completing sulfation of C_{70} at 50, 55, 60, 70 and 80 °C was found to be 28, 22, 16, 12 and 5 h, respectively. With an increase of reaction temperature by only 55 °C, the reaction period was shortened down to 7% of the required time scale for an ambient-temperature reaction. The reaction yield obtained under those conditions was relatively steady in a range of 76–85%, which was rather insensitive to the change of temperature.

An effective sulfation of C_{70} without a prolong reaction period requires a high dose level of P_2O_5 additives as much as 130 equiv. of the C_{70} quantity. Decreasing the amount of P_2O_5 used down to 30 equiv. for a reaction carried out at 60 °C reduced the effective product yield to 47%. Interestingly, we found that the replacement of P_2O_5 by SeO_2 improved significantly the sulfation efficiency of C_{70} . In this case, a 10-fold less in quantity of SeO_2 (3.3 equiv.) was needed for a complete sulfation of C_{70} within 15 h of reaction at 60 °C while maintaining a high product yield of 86%. In fact, by increasing the amount of SeO_2 to 6.0 equiv. of C_{70} applied in the reaction a lower product yield of 4 was obtained owing to, presumably, over-oxidation of the C_{70} molecules that resulted in the formation of unstable intermediates.

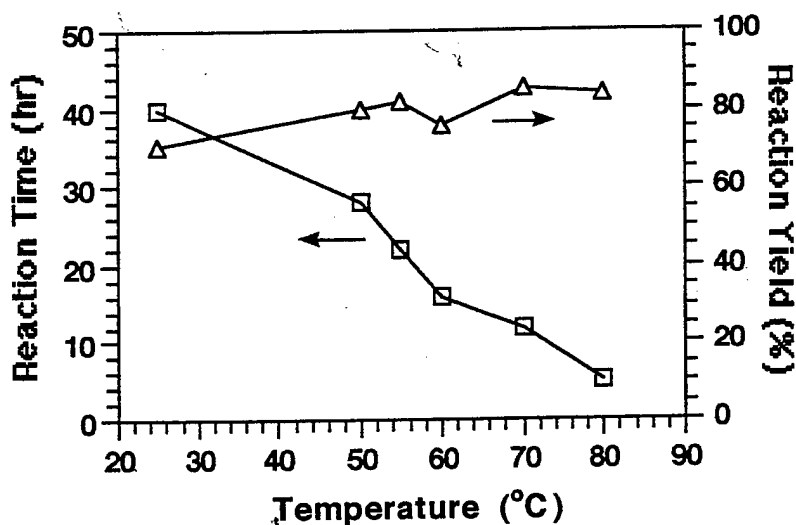


Figure 1: A temperature-dependent sulfation period required for a complete reaction and the yield of the reaction between C_{70} and a reagent mixture of H_2SO_4 - SO_3 - P_2O_5 .

Addition of multiple cyclosulfate moieties onto a C_{70} cage was substantiated by detection of the optical absorptions of the asymmetric and symmetric $RO-SO_2-OR$ stretching bands in the infrared spectrum of **4** at 1424 and 1223 cm^{-1} (Fig. 2b), respectively. The peak position of these two bands as well as the overall spectrum were found to agree well with those (Fig. 2a) reported for hexacyclosulfated C_{60} , $C_{60}(SO_4)_6$, which was synthesized by the reaction of C_{60} with neat oleum in the presence of P_2O_5 .^{5,12} Cyclosulfated **4** is susceptible to partial hydrolysis even under mild conditions of the workup procedures. That resulted in a slight increase in intensity of two broad bands at 1050 and 2480 cm^{-1} , corresponding to optical absorptions of the fullerenolic C-O and sulfatic acid C-SO₃H functional groups, respectively. Hydrolysis of **4** in H_2O at 85 °C gave [70]fullerenols **3**, showing four characteristic broad absorption bands (Fig. 2d) centered at 3271 (—

OH), 1621, 1373, and 1049 ($\text{C}-\text{O}$) cm^{-1} in close resemblance to those obtained for [60]fullerenols (Fig. 2c). Chromatography of the compound **3** on TLC (SiO_2) gave a single spot at $R_f = 0.9$ using a mixture of DMF–MeOH– H_2O /4.0:3.0:0.2 as an eluent.

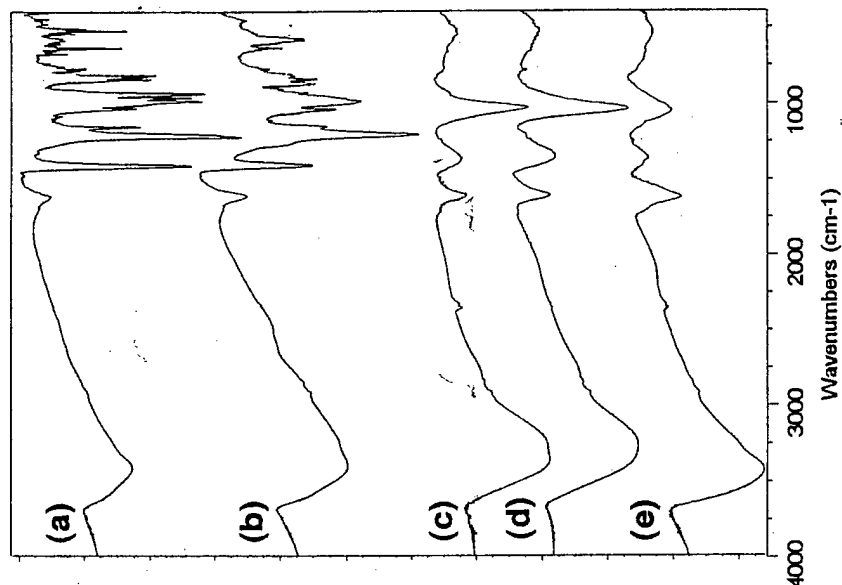


Figure 2: Infrared spectrum of (a) hexacyclosulfated C_{60} **2**, (b) nanocyclosulfated C_{70} **4**, (c) dodecahydroxylated C_{60} **1**, and (d) octadeca-hydroxylated C_{70} **3**, showing disappearance of $\text{RO}-\text{SO}_2-\text{OR}$ stretching bands of **4** at 1424 (ν_{as}) and 1223 (ν_s) cm^{-1} upon hydrolysis.

The relative intensity of these four bands varied slightly upon a variation of workup procedures, as shown in Fig. 3e, where the compound **3** in DMF was reprecipitated and further purified as solids from diethylether. No obvious differences in chemical characteristics were found among these fullerenols. Our hypothesis links this variance in intensity of the fullerenolic IR absorption bands to the difference of the molecular packing of fullerenols in the solid state.

Data from the elemental analyses (EA) of a sample of **4** were found to fit well with a structural formula of $\text{C}_{70}(\text{SO}_4)_8 \cdot 2\text{H}_2\text{O}$ with a deviation of ± 0.4 , 0.02, and 0.13% between the experimental value obtained and theoretical value calculated for the carbon, hydrogen, and sulfur content, respectively. In connection with the EA data, mass spectroscopic studies of **3** were carried out utilizing the matrix-assisted laser desorption ionization (MALDI) technique with a mixture of 2-hydroxyquinoline and 8-hydroxyquinoline as a matrix material. A sample of **3** derived from the parent cyclosulfated C_{70} **4**, synthesized under a sulfation temperature of 60 $^\circ\text{C}$ for 15 h in the presence of oleum– SeO_2 , was used in the measurements.

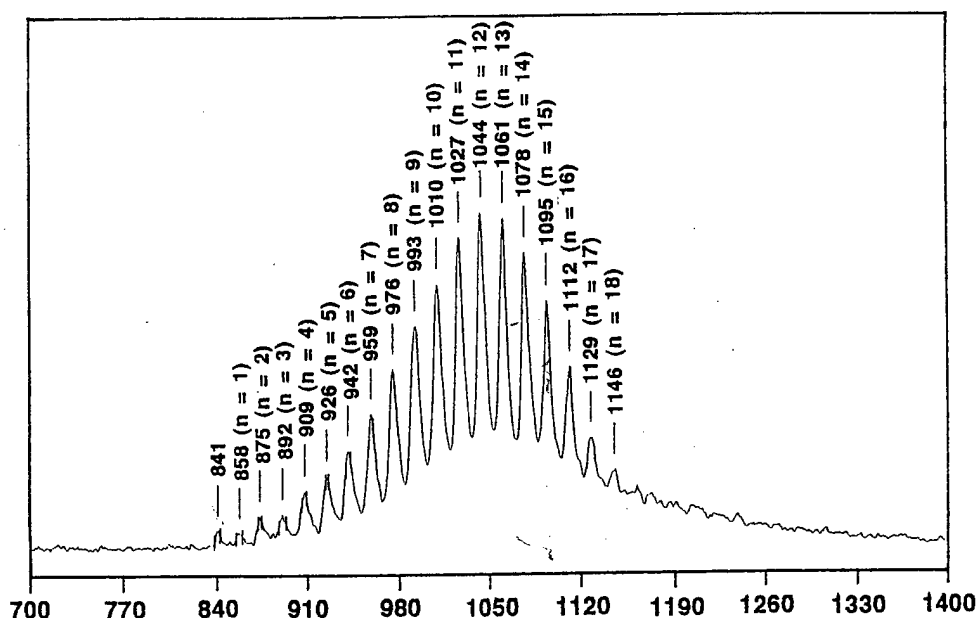


Figure 3: Negative ion MALDI-TOF-MS spectrum of **3**, derived from the parent cyclosulfated C_{70} **4**, using a mixture of 2-hydroxyquinoline and 8-hydroxyquinoline as a matrix material.

Consequently, the MALDI-TOF mass spectrum of **3** displayed a series of mass groups with a well-defined evolution of a nearly constant weight increase in 17 mass units at m/z (the mass of an ion fragmentation with a maximum peak intensity in each group) 858 ($n = 1$), 875 ($n = 2$), 892 ($n = 3$), 909 ($n = 4$), 926 ($n = 5$), 942 ($n = 6$), 959 ($n = 7$), 976 ($n = 8$), 993 ($n = 9$), 1010 ($n = 10$), 1027 ($n = 11$), 1044 ($n = 12$), 1061 ($n = 13$), 1078 ($n = 14$), 1095 ($n = 15$), 1112 ($n = 16$), 1129 ($n = 17$), and 1146 ($n = 18$). Intensity of the next possible ion with a higher mass at m/z 1163 ($n = 19$) is close to or within the background intensity level. It is clear that the detected ion fragmentations, showing the gain of a hydroxy (OH) functional group to the preceding ion fragment, concur with the mass of $C_{70}(OH)_n$ as polyhydroxylated C_{70} derivatives. Detection of the highest ion mass at m/z 1146 indicated that the octadecahydroxylated C_{70} ion, $[C_{70}(OH)_{18}]^-$, could be the molecular ion of [70]fullerenol. This conclusion differs slightly from the data of elemental analyses which revealed the structure of **4** as octacyclosulfated C_{70} . Hydrolysis of it under mild acidic aqueous conditions should, in principle, afford the corresponding hexadecahydroxylated C_{70} . However, by considering data fluctuation occurred in the elemental analyses from sample to sample of **4** owing partially to the incomplete combustion of fullerene cages during the process of microanalyses, the MALDI-TOF-MS data may be better presenting the actual structure of **3** which can be used to correlate the structure of **4** as nonacyclosulfated C_{70} , $C_{70}(SO_4)_9$, instead.

Experimental

General. Pure C_{70} (98%) was purchased from Materials Electrochemical Research (MER) Co. and used as received. Infrared spectra were recorded as KBr pellets on a Nicolet 750 series FT-IR spectrometer. Fuming sulfuric acid, containing 30% of SO_3 , was purchased from Merck Co. and used as received. Matrix-assisted laser desorption ionization (MALDI) mass spectrum was recorded on a HP G2025A MALDI-TOF MS system, using a mixture of 2-hydroxyquinoline and 8-hydroxyquinoline as a matrix material. A N_2 -laser operated at a wavelength of 337 nm was utilized for providing a dissociation energy of roughly 2.50 μJ in the negative ion measurements. During the sample preparation for the MALDI experiments, [70]fullerenols was dissolved in $MeOH-CH_3CN-H_2O$ as a saturated solution. This solution mixture was then acidified by the addition of HCl (1N) in a trace quantity prior to measurements. The final concentration of [70]fullerenols in a sample solution deposited on a MALDI probe was 1000 ppm. Elemental analyses of [70]fullerenols and polycyclosulfated C_{70} were carried out at the Institute of Nuclear Energy Research, Taiwan.

Synthesis of octadecahydroxylated C_{70} (3)

Method 1: C_{70} (150 mg, 0.18 mmol) was partially dissolved in fuming sulfuric acid (5 ml, 30% SO_3) in a reaction flask (50 ml) and stirred at ambient temperatures for 3 min. The mixture was added by P_2O_5 (760 mg, 5.34 mmol, 30 equiv.) and treated momentarily under ultrasonic conditions for 5 min. It was then stirred at 60 °C under N_2 for 15 h to give a light brown solution with suspended bright orange microcrystalline solids. At the end of reaction, the resulting mixture was added dropwise onto crashed ice with vigorous stirring to effect the complete precipitation of the brownish orange products. Sudden increase of temperature should be avoided to minimize partial hydrolysis of the cyclosulfated C_{70} products. Precipitated solids were separated from the acid solution by the centrifuge technique. Solids obtained were repeatedly washed and centrifuged with cold $H_2SO_4-H_2O$ 1:7 (3 x 10 ml) and partially dried in vacuum at 40 °C for 2 h. It was further washed with CH_3CN (distilled over CaH_2 , 4 x 5 ml) and dried in vacuum at 40 °C to afford the orange to brownish red solids of polycyclosulfated C_{70} 4 (120 mg, 47% based on a nonacyclosulfated C_{70} product structure).

Method 2: C_{70} (150 mg, 0.18 mmol) was partially dissolved in fuming sulfuric acid (5 ml, 30% SO_3) in a reaction flask (50 ml) and stirred at ambient temperatures for 3 min. The mixture was

added by SeO_2 (65 mg, 0.58 mmol, 3.3 equiv.) and treated momentarily under ultrasonic conditions for 5 min. It was then stirred at 60 °C under N_2 for 15 h to give a light brown solution with suspended bright orange microcrystalline solids. The workup procedure followed the one described in the method 1. Dark brownish red solids of polycyclosulfated C_{70} **4** (220 mg, 86% based on a nonacyclosulfated C_{70} product structure) were obtained. IR (KBr) ν_{max} 3400 (br), 2920w, 2848w, 1622w, 1424 (SO_2), 1233s (SO_2), 1170, 1055, 1003s, 945, 885, 852, 831w, 779w, 642, 593, 580, and 458w cm^{-1} , consistent with those reported previously.^{5,12} UV-Vis (DMF): $\lambda_{\text{max}} = 275$ nm. Anal. Calcd for $\text{C}_{70}\text{H}_4\text{S}_8\text{O}_{34}$ as $\text{C}_{70}(\text{SO}_4)_8 \cdot 2\text{H}_2\text{O}$: C, 51.09; H, 0.24; S, 15.57; O, 33.09. Found: C, 50.70; H, 0.22; S, 15.70.

A reaction flask (50 ml) equipped with a condenser and an inert gas bubbler was charged with cyclosulfated C_{70} **4** (150 mg, 0.11 mmol) and distilled water (5 ml). The pH of the solution was measured to be 2.0. The mixture was stirred at 80 °C under N_2 for 24 h to give a dark brown suspension. At the end of hydrolysis, the pH of the solution was measured to be 1.0. The resulting suspended solids were separated from the aqueous solution by centrifuge. It was repeatedly washed and centrifuged with water (3 x 15 ml) and dried in vacuum at 40 °C to afford brown solids of octadecahydroxylated C_{70} **3** ([70]fullerenols, 90 mg, 72%). IR (KBr) ν_{max} 3271s (br, OH), 1621 (br), 1373 (br), 1049s (C–O), 539, and 468 cm^{-1} . UV-Vis (DMF): $\lambda_{\text{max}} = 285$ nm. MALDI-TOF mass spectrum m/z (negative ion, mass of the highest ion peak in the fragmentation group) 858 ($n = 1$), 875 ($n = 2$), 892 ($n = 3$), 909 ($n = 4$), 926 ($n = 5$), 942 ($n = 6$), 959 ($n = 7$), 976 ($n = 8$), 993 ($n = 9$), 1010 ($n = 10$), 1027 ($n = 11$), 1044 ($n = 12$), 1061 ($n = 13$), 1078 ($n = 14$), 1095 ($n = 15$), 1112 ($n = 16$), 1129 ($n = 17$), 1146 ($n = 18$), and 1163 (w). Owing to a variable, high hydrated water content in solids of **3**, data of the elemental analyses (C, H and O) fluctuated from sample to sample.

Acknowledgment. The authors thank Dr. L. C. Men of the Institute of Nuclear Energy Research, Taiwan for the chemical analyses of compounds. This work was supported by AOARD/AFOSR under the grant no. FQ8671-9601280.

References

1. Chiang, L.Y.; Upasani, R.B.; Swirczewski, J.W. *J. Am. Chem. Soc.* **1992**, *114*, 10154.
2. Chiang, L.Y.; Bhonsle, J.B.; Wang, L.Y.; Shu, S.F.; Chang, T.M.; Hwu, J.R. *Tetrahedron* **1996**, *52*, 4963.

3. Schneider, N.S.; Darwish, A.D.; Kroto, H.W.; Taylor, R.; Walton, D.R.M. *J. Chem. Soc., Chem. Commun.* **1994**, 15.
4. Li, J.; Takeuchi, A.; Ozawa, M.; Li, X.; Saigo, K.; Kitazawa, K. *J. Chem. Soc., Chem. Commun.* **1993**, 1784.
5. Chiang, L.Y.; Wang, L.Y.; Swirczewski, J.W.; Soled, S.; Cameron, S. *J. Org. Chem.* **1994**, 59, 3960.
6. Chiang, L.Y.; Wang, L.Y.; Tseng, S.M.; Wu, J.S.; Hsieh, K.H. *J. Chem. Soc., Chem. Commun.* **1994**, 2675.
7. Chiang, L.Y.; Wang, L.Y.; Kuo, C.S. *Macromolecules* **1995**, 28, 7574.
8. Wang, L.Y.; Wu, J.S.; Kuo, C.S.; Tseng, S.M.; Hsieh, K.H.; Chiang, L.Y. *J. Polym. Res.* **1996**, 3, 1.
9. Chiang, L.Y.; Lu, F.J.; Lin, J.T. *J. Chem. Soc., Chem. Commun.* **1995**, 1283.
10. Tsai, M.C.; Chen, Y.H.; Chiang, L.Y. *J. Pharmacy and Pharmacology* **1997**, 49, 438.
11. Lai, Y.L.; Chiang, L.Y. *J. Autonomic Pharmacology* **1997**, 17, 229.
12. Chen, B.H.; Huang, J.P.; Wang, L.Y.; Shiea, J.; Chen, T.L.; Chiang, L.Y. *J. Chem. Soc., Perkin Trans. I* (accepted, in press).